First observation of the decay $K^+ \to e^+ \nu_e \mu^+ \mu^-$

H. Ma,[1] R. Appel,[6,3] G. S. Atoyan,[4] B. Bassalleck,[2] D. R. Bergman,[6,*] N. Cheung,[3] S. Dhawan,[6] H. Do,[6] J. Egger,[5] S. Eilerts,[2,†] W. Herold,[5] V. V. Issakov,[4] H. Kaspar,[5] D. E. Kraus,[3] D. M. Lazarus,[1] P. Lichard,[3] J. Lowe,[2] J. Lozano,[6,‡] W. Majid,[6,§] S. Pislak,[7,6,‖] A. A. Poblaguev,[4] P. Rehak,[1] A. Sher,[3,¶] J. A. Thompson,[3,**] P. Truöl,[7,6] and M. E. Zeller[6]

[1]*Brookhaven National Laboratory, Upton, New York 11973, USA*
[2]*Department of Physics and Astronomy, University of New Mexico, Albuquerque, New Mexico 87131, USA*
[3]*Department of Physics and Astronomy, University of Pittsburgh, Pittsburgh, Pennsylvania 15260, USA*
[4]*Institute for Nuclear Research of Russian Academy of Sciences, Moscow 117 312, Russia*
[5]*Paul Scherrer Institut, CH-5232 Villigen, Switzerland*
[6]*Physics Department, Yale University, New Haven, Connecticut 06511, USA*
[7]*Physik-Institut, Universität Zürich, CH-8057 Zürich, Switzerland*

(Received 12 May 2005; published 7 February 2006)

Experiment 865 at the Brookhaven AGS has observed the decay $K^+ \to e^+ \nu_e \mu^+ \mu^-$. The branching ratio extracted is $(1.72 \pm 0.37(\text{stat}) \pm 0.17(\text{syst}) \pm 0.19(\text{model})) \times 10^{-8}$ where the third term in the error results from the use of a model to extrapolate into a kinematic region dominated by background.

DOI: 10.1103/PhysRevD.73.037101 PACS numbers: 13.20.Eb, 13.40.Ks

The internally converted, radiative K_{l2} decays, $K^+ \to l^+ \nu l'^+ l'^-$, are an important source of information on the kaon. For example, within the framework of Chiral Perturbation Theory (ChPT) [1] radiative kaon decays can serve both as an important test and a source of input parameters for the theory.

The $K^+ \to l^+ \nu l'^+ l'^-$ is described by the graphs of Fig. 1. The tree diagrams (a) and (b) are the inner bremsstrahlung (IB), where the virtual photon is radiated by the kaon or positron. This contribution is electron-helicity suppressed and is negligible for the decay $K^+ \to e^+ \nu \mu^+ \mu^-$. The short distance, structure-dependent (SD) terms are combined in graph (c). The SD contribution is characterized by form factors F_V, F_A, and R, which we define in accordance with the Particle Data Group [2]. These may be functions of W^2 and q^2, the invariant masses of the $e^+\nu$ and the $\mu^+\mu^-$ pairs, respectively. In the vector meson dominance picture [3], this dependence has the form

$$F_V(q^2, W^2) = F_V(0,0)/[(1 - q^2/m_\rho^2)(1 - W^2/m_V^2)] \quad (1)$$

with similar expressions for F_A and R. Here, m_ρ is the ρ-meson mass and m_V is the mass of the $K^*(892)$ for F_V and of the $K^*(1270)$ for F_A and R. ChPT relates the form factors F_V and F_A to those of the $\pi \to e\nu\gamma$ decay and form factor R to the kaon charge radius. Bijnens *et al.* [4] gave a ChPT prediction for the $K^+ \to e^+ \nu \mu^+ \mu^-$ branching ratio of 1.12×10^{-8}. The previous experimental limit was $<5.0 \times 10^{-7}$ [2,5].

Experiment E865 at the Brookhaven National Laboratory Alternating Gradient Synchrotron (AGS) has produced substantial improvements in our knowledge of these radiative decays. Results for the decays $K^+ \to \mu^+ \nu e^+ e^-$ and $K^+ \to e^+ \nu e^+ e^-$ have already been reported [6]. This paper presents results from E865 for the first observation of the decay $K^+ \to e^+ \nu \mu^+ \mu^-$.

The experimental apparatus for Brookhaven E865 is shown in Fig. 2 and has been described in detail elsewhere [7]. A 6 GeV/c unseparated beam from the AGS was incident on a 5-m long evacuated decay volume. Decay particles from this region were separated into positive and negative charges by a dipole magnet and were momentum-analyzed by a spectrometer containing a second dipole magnet and four 4-view wire chambers, P1–P4. Particle identification was provided by two pairs of gas Cherenkov counters, C1 and C2 (hydrogen on the negative-particle side and methane on the positive side), a 30×20-element Shashlyk calorimeter containing 15 radiation lengths of lead/scintillator sandwich, and a muon detector containing 12 layers of iron with 12 2-view wire chambers interspersed. Additionally, there were 4 hodoscope planes, A–D, for timing and triggering. A 12(horizontal) $\times$ 32(vertical)-element pixel detector, with pixel size 7×7 mm, was located in the incident kaon beam to determine

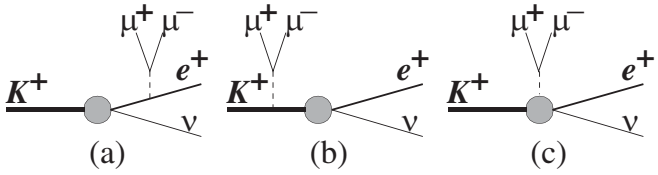

FIG. 1. Graphs for contributions to $K^+ \to e^+ \nu \mu^+ \mu^-$.

*Present address: Rutgers University, Piscataway, NJ 08855., USA
†Present address: Black Mesa Capital, Santa Fe, NM 87501., USA
‡Present address: University of CT, Storrs, CT 06269., USA
§Present address: LIGO/Caltech, Pasadena, CA 91125., USA
‖Present address: Phonak AG, CH-8712 Stäfa, Switzerland.
¶University of CA, Santa Cruz, CA 95064., USA
**Deceased.

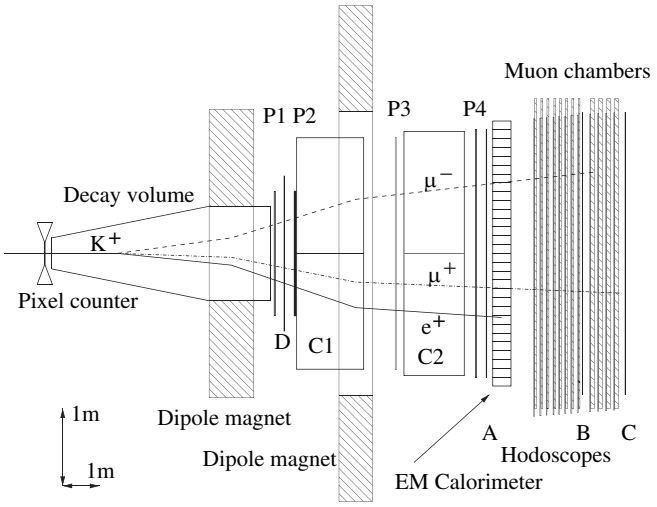

FIG. 2. Plan view of the experimental apparatus for E865.

the position of the decaying kaon at the entrance to the decay volume.

The data taking for this part of E865 took place in parallel with studies of the $K^+ \to \pi^+\pi^- e^+\nu$ (K_{e4}) and $K^+ \to \pi^+\mu^+\mu^-$ decays, which have already been published [8–10].

Selection of candidate events required three tracks giving a vertex z-coordinate within the decay region and an acceptable value of S, where S^2 is the sum of squares of the deviations of the three tracks from the fitted vertex. Also, the individual tracks were each required to have good χ^2 for the reconstruction and good timing. Electron identification required signals in both positive side Cherenkov detectors and an energy deposition in the calorimeter equal to the reconstructed track momentum. The above cuts were also used in the event selection for the K_{e4} analysis. Additionally, for $K^+ \to e^+\nu\mu^+\mu^-$, the muon candidate tracks were required to have sufficient hits in the muon wire chambers, a hit in the appropriate element of the B hodoscope, located in the middle of the muon stack, and a signal consistent with minimum ionizing in the shower calorimeter.

For each event, the neutrino momentum was calculated from the missing momentum; $\mathbf{p}_\nu = \mathbf{p}_{K^+} - \mathbf{p}_{\mu^+} - \mathbf{p}_{\mu^-} - \mathbf{p}_{e^+}$. The magnitude of $\mathbf{p}_{K^+}$ was taken as the average value, derived from measurements of pion momenta from $K_{3\pi}$ decays. The direction of $\mathbf{p}_{K^+}$ was determined from the beam pixel detector and the reconstructed vertex where possible. About 45% of events had an unambiguous hit in the beam pixel detector. For those events that did not, the average kaon beam direction was assumed in the event reconstruction.

Simulation of the experiment was carried out using the GEANT package [11]. A problem with this package is that pion interactions are not always well simulated. As a result, the probability that a pion can penetrate well into the muon stack, causing it to be misidentified as a muon, is not well determined by the simulation. Experimental studies using $K^+ \to \pi^+\pi^0$, $K^+ \to \pi^0\mu^+\nu$ (each followed by $\pi^0 \to \gamma e^+ e^-$) and $K^+ \to \pi^+\pi^+\pi^-$ events established that this π to μ misidentification probability is calculated by the simulation with an uncertainty of about 10%.

With the above cuts, 1834 candidate events remain. These are shown in Fig. 3 as a scatter plot of $m_{e^+\mu^+\mu^-}$ against $m_{e^+\nu\mu^+\mu^-}$, which also shows the region of $m_{e^+\nu\mu^+\mu^-}$ where genuine events are expected.

Three sources of background were considered:

(a) $K^+ \to \pi^+\pi^- e^+\nu$ (K_{e4}) with both pions misidentified as muons,

(b) Accidentals, and

(c) $K^+ \to \pi^+\pi^+\pi^-$ ($K_{3\pi}$) with the pions misidentified as e^+, μ^+ and μ^- respectively.

The contributions from these were determined as follows.

K_{e4} events give the largest contribution to the background. A large sample of Monte Carlo events (6×10^7, equivalent to 20 times the number of data events) was generated. Background hits taken from actual data events were added to the simulated events, and the sample was analyzed as for data events. This procedure should give a realistic estimate of the background shape. The magnitude of he K_{e4} background has an error due to uncertainty in the π to μ misidentification probability, which is about 0.05 with an error of $\sim$10%.

A sample of accidental events was extracted from the data by selecting events with bad timing and badly reconstructed vertices. The reconstructed total charged-track momenta for these events shows a tail above 6.5 GeV/c. The total charged-track momentum spectrum for the $K^+ \to e^+\nu\mu^+\mu^-$ candidates shows a similar tail, which is assumed to arise entirely from accidentals. Therefore, the background contribution from accidentals was assumed to have the same shape as the bad-timing, bad-vertex events, with a magnitude derived by scaling this high-momentum tail to match that in the data.

The background contribution from $K_{3\pi}$ decays was estimated by examining the $K^+ \to \pi^+\pi^+\pi^-$ data events

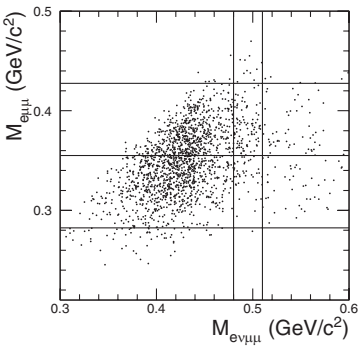

FIG. 3. Scatter plot of $m_{e^+\mu^+\mu^-}$ against $m_{e^+\nu\mu^+\mu^-}$ for candidate $K^+ \to e^+\nu\mu^+\mu^-$ events. Valid events lie in the band $m_{e^+\nu\mu^+\mu^-} \sim m_K$ indicated on the plot.

obtained from the minimum-bias trigger. The μ^+ and μ^- identification was required but there was no particle identification requirement on the third particle. The sample was then scaled by the known π^+ to e^+ misidentification probability of 1.3×10^{-3}, determined from a study of K_{e4} events, where the contamination from $K_{3\pi}$ decays is easily identified by the kinematics of the 3π final state.

Background from $K^+ \to \pi^+\pi^-\mu^+\nu$ is negligible because of the small π^+ to e^+ misidentification probability (1.3×10^{-3}) and the low branching ratio for this decay.

The three sources of background are shown as plots of $m_{e^+\mu^+\mu^-}$ against $m_{e^+\nu\mu^+\mu^-}$ in Fig. 4, which also shows the simulated $K^+ \to e^+\nu\mu^+\mu^-$ signal. The signal appears as a peak in $m_{e\nu\mu\mu}$ at the kaon mass, 0.494 GeV/c^2, the region indicated by the vertical lines in Figs. 3 and 4. It is also apparent from Fig. 4, that the signal-to-background ratio will be best for high values of $m_{e\mu\mu}$.

Because the signal-to-background ratio becomes poor at low $m_{e\mu\mu}$, it is difficult to extract significant information on form factors from the present experiment. Initially, therefore, we assumed form factors for $K^+ \to e^+\nu\mu^+\mu^-$ in order to extrapolate the signal into regions where it is not observable, to extract the total branching ratio. To do so, the 2-dimensional plot, Fig. 3, was fitted with the sum of the signal and background contributions shown in Fig. 4. While the magnitude of the signal was a free parameter in the fit, the shape of the signal distribution was fixed by the form factors F_A, F_V and R, whose values are taken from the E865 measurements on $K^+ \to e^+\nu e^+e^-$ and $\mu^+\nu e^+e^-$ [6]:

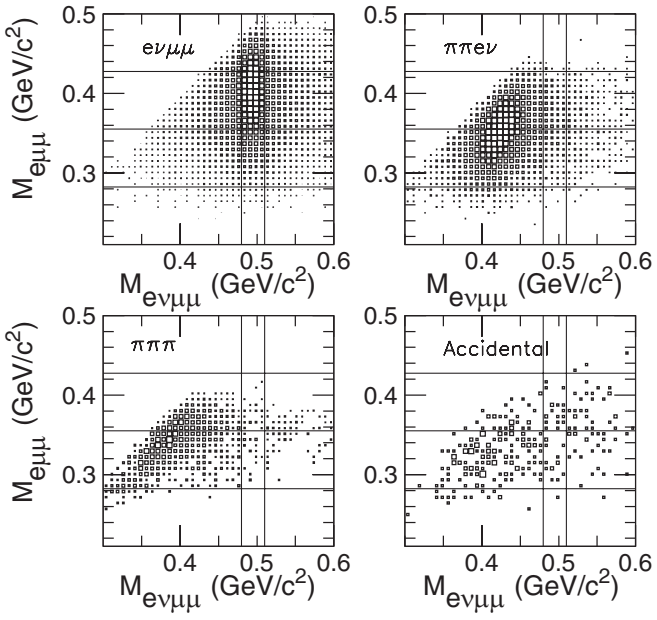

FIG. 4. Simulation results for the $K^+ \to e^+\nu\mu^+\mu^-$ (top left-hand plot) and the computed contributions from the three background sources, K_{e4}, $K_{3\pi}$ and accidentals.

$$F_V(0,0) = 0.112 \pm 0.018, \quad (2)$$

$$F_A(0,0) = 0.035 \pm 0.019, \quad (3)$$

$$R(0,0) = 0.227 \pm 0.019. \quad (4)$$

Since the K_{e4} contribution to the background is uncertain to about 10%, we allow the magnitude of it to float in the fitting.

The fit is shown in Fig. 5 as a projection onto the $m_{e\nu\mu\mu}$ axis of the fit and of the data from Fig. 3. The three contributions to the background are shown separately. Figure 6 shows the same projection for events in three bands of $m_{e\mu\mu}$ as follows:

Figure 6(a): $0.2825 < m_{e\mu\mu} < 0.355$ GeV/c^2,

Figure 6(b): $0.355 < m_{e\mu\mu} < 0.4275$ GeV/c^2,

Figure 6(c): $m_{e\mu\mu} > 0.4275$ GeV/c^2.

These regions are indicated by the horizontal lines in Figs. 3 and 4. Figure 6(c) contains 24 data events with a fitted background of 6.9 events, and Fig. 6(b) has 176 events with a background of 133 ± 4 events for the reconstructed kaon mass range $0.465 < m_{e\nu\mu\mu} < 0.540$ GeV/c^2.

The fit resulted in a branching ratio, B, of

$$B = (1.72 \pm 0.37(\text{stat}) \pm 0.17(\text{formfactor}) \pm 0.09(\text{slope}) \pm 0.17(\text{syst})) \times 10^{-8} \quad (5)$$

The K_{e4} decay was used as a normalization channel for the analysis. Thus the systematic error arises predominantly from uncertainties in simulation of the muon detection efficiency since muons are not involved in K_{e4}. For this, we estimate $\pm 10\%$. Additional errors arise from uncertainties in the form factors of Eqs. (2)–(4), and also in the slopes of the q^2 and W^2 dependence of these form factors. For this contribution, we assume, as in Ref. [6], that these

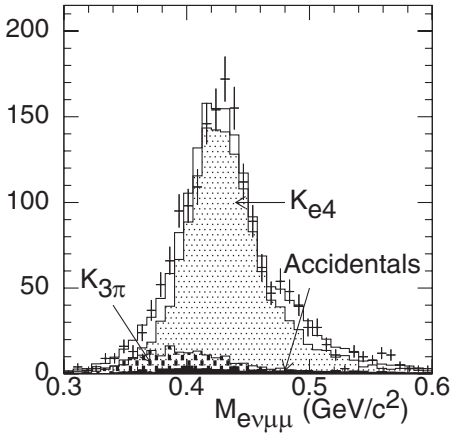

FIG. 5. Projection onto the $m_{e\nu\mu\mu}$ axis of the data of Fig. 3 (points) and of the fitted distribution (unshaded histogram). The three background contributions are shown separately (shaded histograms).

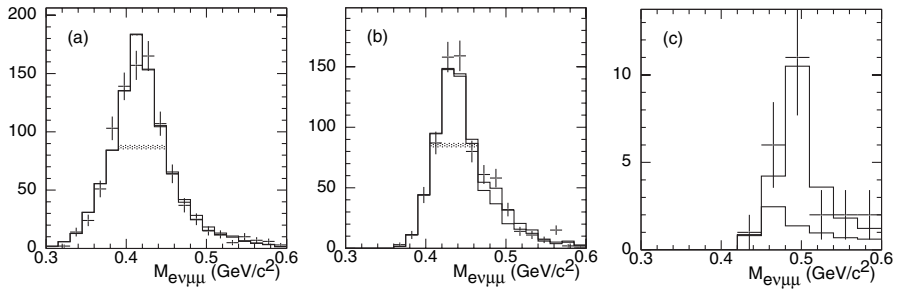

FIG. 6. Distribution in $m_{e\nu\mu\mu}$ of events in three bands of $m_{e\mu\mu}$: (a) $0.2825\ \mathrm{GeV}/c^2 < m_{e\mu\mu} < 0.355\ \mathrm{GeV}/c^2$, (b) $0.355\ \mathrm{GeV}/c^2 < m_{e\mu\mu} < 0.4275\ \mathrm{GeV}/c^2$ and (c) $m_{e\mu\mu} > 0.4275\ \mathrm{GeV}/c^2$. The points are the experimental data and the histogram is the fitted spectrum. The shaded areas show the fitted background contribution.

slopes are uncertain to $\pm 30\%$. The fit gave $\chi^2 = 132$ for 112 degrees of freedom. The best fit resulted in a scaling factor for the K_{e4} background of 0.86 ± 0.02 which is consistent with the estimated uncertainty in the π to μ misidentification probability of about 10%. Combining the errors in quadrature gives

$$B = (1.72 \pm 0.45) \times 10^{-8}. \quad (6)$$

A study of the statistical significance of the background function shows that, in fitting the entire $m_{e\mu\mu}$ *vs.* $m_{e\nu\mu\mu}$ distribution, the probability of a statistical fluctuation in the background simulating the signal is $<10^{-6}$.

If F_A, F_V and R are all allowed to vary in the fitting, the resulting values for B, F_A, F_V and R are consistent with Eqs. (2)–(5) but with substantially larger errors. This is the expected consequence of the variation of signal-to-background ratio across the range of phase space covered by our data. However, since R is the dominant term, a fit was carried out with R varied, with F_A and F_V constrained at the values of Eqs. (2) and (3). This fit gave

$$R(0, 0) = 0.303 \pm 0.036(\mathrm{stat}) \pm 0.011(\mathrm{form\ factor}) \pm 0.009(\mathrm{slope}) \pm 0.017(\mathrm{syst}). \quad (7)$$

This is consistent with Eq. (4) at the 1.7-standard-deviation level, and although our results cannot improve our knowledge of the form factors, they can at least demonstrate consistency with the values from the $K^+ \to l^+ \nu e^+ e^-$ data.

The result for B can be compared with the ChPT prediction of Bijnens *et al.* [4] of 1.12×10^{-8}. If the form factors of Eqs. (2)–(4) are used in the theoretical calculation, the prediction becomes $B = (1.04 \pm 0.15) \times 10^{-8}$ which is consistent with our result at the 1.5 standard-deviation level.

In summary, we have made a first observation of the decay $K^+ \to e^+ \nu \mu^+ \mu^-$ and have determined the branching ratio to 25%. We find values for the form factors that are consistent with those for other $K^+ \to l^+ \nu l'^+ l'^-$ decays but with less accuracy. The branching ratio is reasonably consistent with a ChPT prediction.

We gratefully acknowledge the contributions to the success of this experiment by the staff and management of the AGS at the Brookhaven National Laboratory, and the technical staffs of the participating institutions. This work was supported in part by the U. S. Department of Energy, the National Science Foundations of the USA, Russia and Switzerland, and the Research Corporation.

[1] S. Weinberg, Physica A (Amsterdam) **96**, 327 (1979); J. Gasser and H. Leutwyler, Ann. Phys. (N.Y.) **158**, 142 (1984); Nucl. Phys. **B250**, 465 (1985).
[2] S. Eidelman *et al.*, Phys. Lett. B **592**, 1 (2004).
[3] D. Bardin and E. Ivanov, Sov. J. Part. Nucl. **7**, 286 (1976).
[4] J. Bijnens, G. Ecker, and J. Gasser, Nucl. Phys. **B396**, 81 (1993).
[5] S. Adler *et al.*, Phys. Rev. D **58**, 012003 (1998).
[6] A. A. Poblaguev *et al.*, Phys. Rev. Lett. **89**, 061803 (2002).
[7] R. Appel *et al.*, Nucl. Instrum. Methods Phys. Res., Sect. A **479**, 349 (2002).
[8] S. Pislak *et al.*, Phys. Rev. Lett. **87**, 221801 (2001).
[9] S. Pislak *et al.*, Phys. Rev. D **67**, 072004 (2003).
[10] H. Ma *et al.*, Phys. Rev. Lett. **84**, 2580 (2000).
[11] GEANT Detector description and simulation tool, CERN Program Library, Long Writeup W5013 (1994).